ACS APPLIED MATERIALS & INTERFACES

Research Article

www.acsami.org

Viable Method for the Synthesis of Biphasic TiO_2 Nanocrystals with Tunable Phase Composition and Enabled Visible-Light Photocatalytic Performance

Ramireddy Boppella, Pratyay Basak, and Sunkara V Manorama*

Nanomaterials Laboratory, Inorganic & Physical Chemistry Division, Indian institute of Chemical Technology, Hyderabad, Andhra Pradesh, India

Supporting Information

ABSTRACT: Here we demonstrate a facile method to synthesize high-surface-area TiO_2 nanoparticles in aqueous-ethanol system with tunable brookite/rutile and brookite/anatase ratio possessing high surface area that exhibits enhanced photoactivity. Titanium tetrachloride ($TiCl_4$) is used as the metal precursor of choice and the tuning of phase compositions are achieved by varying the water:ethanol ratio, used as mixed solvent system. The synthesized samples were characterized in detail using X-ray diffraction (XRD), Raman spectroscopy, transmission electron microscopy (TEM), BET nitrogen sorption measurements, and UV−vis diffuse reflectance spectroscopy (UV-DRS). The photocatalytic activity of biphasic TiO_2 nanocrystals was evaluated by following the degradation kinetics of rhodamine-B dye in aqueous solution and under visible light. Mixed-phase TiO_2 nanostructures composing 83% brookite and 17% of rutile exhibited superior photoactivity when compared to Degussa P25 and phase-pure anatase nanocrystals. The exceptional photocatalytic activity of the synthesized nanostructures can be elucidated on the account of their large surface area and biphasic composition. On the basis of the detailed investigation reported herein, we conclude that tuning the ethanol volume in the mixed-solvent reaction system holds the key to tailor and control the final TiO_2 phase obtained.

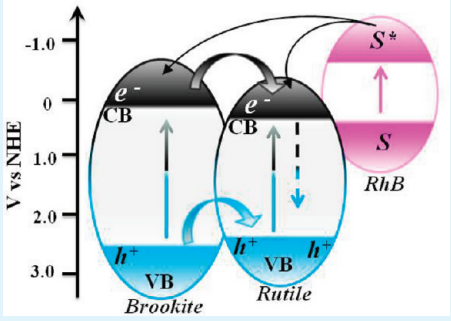

KEYWORDS: *titanium dioxide, biphasic, photocatalyst, thermal hydrolysis*

1. INTRODUCTION

Over the past decade, nanocrystalline titanium dioxide has been one of the most studied materials envisaged to address many environmental and global issues; this includes harnessing solar energy (photovoltaic and water splitting devices).[1−3] The three well-known polymorphs of TiO_2 are rutile (tetragonal), anatase (tetragonal), and brookite (orthorhombic). It is now clearly established that the photo activity of TiO_2 depends on its physicochemical properties such as crystallite size, surface area, porosity, morphology and phase compositions.[4−7] Owing to its high photocatalytic activity, anatase is the most studied among the three phases and this is primarily because of its moderate ability to suppress the recombination of photogenerated hole and electron pairs.[8,9] In some aspects, it has been contended that nanosized rutile titania shows better performance as an electrode material than anatase.[10] Improving on the light trapping capability can enhance the photoactivity of TiO_2 multifold and the accepted approach to do so is stretching the optical band edge (band gap tuning) of TiO_2 from the UV into visible region. Among several methods that have been developed to achieve this modification of the energy levels, one of the most popular practices is to introduce new intermediate energy levels between the valence and conduction bands. Another efficient method is to blend complementary phases to achieve the desired absorption in the visible range exploiting irreversible charge transfer mechanism from one phase to the other, leading to efficient photoactivity.

In this perspective, TiO_2 photocatalysts composed of mixed phases have attracted significant attention, as they can exhibit superior catalytic activity compared to either of the constituent pure phases. Most of the studies have helped to establish the fact that the photocatalytic efficiency is enhanced by the existence of a synergistic effect between two phases, which effectively prevents the recombination of photo generated electrons and holes.[11] The most popular example is Degussa P25 consisting of 80% anatase and 20% rutile, which is now the accepted benchmark for comparative evaluation of titania as photocatalyst. The enhancement of activity for Degussa P25 is attributed to the transfer of photo excited electron from high energy anatase to lower energy rutile at the junction formed between these two types of crystalline lattices. This effectively retards the recombination rate within anatase leading to further electron−hole separation and hence, improved photocatalytic activity.[12] Attempts to synthesize mixtures of TiO_2 nanocrystals consisting of biphasic anatase-rutile, anatase-brookite, rutile-brookite and triphasic anatase-rutile-brookite for higher photo-

Received: October 3, 2011
Accepted: February 17, 2012
Published: February 17, 2012

activity than pure anatase, brookite, or rutile have been reported by several researchers.[13−16] Nevertheless, in comparison with anatase and rutile, brookite is the least studied polymorph although it exhibits reasonably good photocatalytic activity, justifiably because of the challenge in synthesizing it in phase-pure form or under controlled conditions.[17]

Herein, we report a convenient one-pot synthesis of highly active mixed phase TiO_2 nanocrystals with a tunable control on phase composition predominantly comprising brookite. The synthesis was achieved under mild experimental conditions by thermal hydrolysis of $TiCl_4$ as the metal-precursor of our choice in aqueous-ethanol mixed solvent media, without using any additional thermal treatment postsynthesis. Extensive characterizations and supporting analysis justifies our contention that the method is simple, can be appropriately tuned, and is scalable and hence economically feasible. The findings demonstrate that impressive control on formation of phase-pure anatase and/or biphasic mixture of brookite/anatase, brookite/rutile can be exercised by simple variation of water:ethanol ratio in the mixed solvent system. The photocatalytic performances of synthesized samples are assessed for Rhodamine B, as a model system and the degradation kinetics are comparatively evaluated against commercially available Degussa P25 taken as reference.

2. EXPERMENTAL SECTION

2.1. Chemicals and Materials. Titanium tetrachloride ($TiCl_4$) and absolute ethanol (99.9%) from SD fine chemicals, India. Rhodamine B was obtained from Merck. All the chemicals were used as received without further purification. Milli-Q deionized water (18MΩ) was used for carrying out all the experiments.

2.2. Synthesis. A series of seven titania samples were prepared by thermal hydrolysis method at 373 K. For a typical synthesis, 2 mL of titanium tetrachloride was added slowly to a 70 mL water/ethanol (v/v) mixture at room temperature, which instantly turned into a white turbid solution. During the addition, evolution of a colorless gas, presumed to be mostly HCl and EtCl in significant amount was observed, as a consequence of the $TiCl_4$ hydrolysis/alcoholysis. The suspension was refluxed at 373 K for 16 h under constant stirring. The white precipitate formed was collected and washed with ethanol several times followed by centrifugation (21000 rpm for 15 min) and subsequently dried at 333 K overnight. Depending on the mixed solvent composition for $TiCl_4$ dilution, i.e. water to ethanol volume ratio 7:0, 6:1, 5:2, 4:3, 3:4, 2:5, and 1:6 the samples were labeled as T1,T2, T3, T4, T5, T6, and T7, respectively. No precipitate was observed when pure ethanol was used as the medium.

2.3. Characterization. Powder X-ray diffraction (XRD) patterns were recorded on a Seimens (Cheshire,UK) D5000 X-ray Diffractometer over a 2θ range of 2° to 65° using CuKα (λ = 1.5406 Å) monochromatic radiation source to identify the crystal phase, composition and estimate the crystallite size. Transmission electron microscope (TEM) (Philips Tecnai FEI F20, operating at 200 kV) was used to investigate the morphology and size of the particles. The samples for TEM analysis were prepared by dispersing the material in water by ultrasonication followed by drop-dry loading onto a carbon-coated copper grid. The Raman spectra of the samples were measured on a HORIBA Jobin Yvon Raman Spectrometer, equipped with an excitation source of He−Ne laser (632.8 nm), CCD camera and a scan resolution held at 2 cm^{-1}. The Brunauer−Emmett−Teller (BET) surface area of the samples was estimated by N_2 physi-sorption at liquid nitrogen temperature on a Quantachrome Nova 4000e apparatus. Prior to the measurements, all the samples were pretreated in vacuum at 100 °C for 1 h. UV-DRS spectra were recorded on a Varian UV−vis spectrometer in the wavelength range of 200 − 800 nm. The samples under study were diluted with KBr and the data collected was referenced to a pure KBr pellet. Room temperature photoluminescence was measured on Spex Fluorolog-3 (HORIBA JOBIN YVON) spectrometer.

2.4. Measurement of Photoactivity. The photocatalytic activity of the as prepared mixed phase nanocrystalline TiO_2 was evaluated by the photo assisted degradation of Rhodamine B (RhB) aqueous solution at room temperature under Visible light. A 400 W white lamp (>430 nm, High pressure Hg vapor lamp, SAIC, India) was used as the light source in an indigenously fabricated photo reactor, cooled with flowing water in a cylindrical glass jacket around the lamp. In a typical reaction, 0.03 g of catalyst was dispersed into 30 mL of aqueous RhB (30 mg/L) in the glass reactor vessel. Prior to irradiation, the suspension was magnetically stirred for 30 min in dark to stabilize and equilibrate the adsorption of RhB on the surface of nanocrystalline TiO_2. The stable aqueous dye-TiO_2 suspension was then exposed to visible light irradiation under continual stirring. Five ml aliquots were withdrawn at regular time intervals to carry out the constituent analysis. Centrifugation at 21 000 rpm for 10 min, repeated 3 times on Kubota refrigerated centrifuge was effectively used to separate the suspended titania particles from the aliquots. The concentration of RhB (C/C_O) was estimated using UV−vis spectroscopy. The degradation of RhB post reaction was confirmed using liquid chromatography results (see Figure S2a,b in the Supporting Information) The intensity of the main absorption peak of RhB dye solution at 556 nm (λ_{max}) was followed and the equilibrated RhB and titania concentration in dark was taken as the initial concentration (C_O). A blank run without TiO_2 (RhB), a control experiment using the commercially available Degussa P25 (P25) and reaction in dark on T3 (dark) were carried out under similar conditions for reference and comparative evaluation, respectively.

3. RESULTS AND DISCUSSION

Figure 1 is the XRD data of the as synthesized samples of TiO_2 obtained by thermal hydrolysis of $TiCl_4$ at different H_2O:EtOH

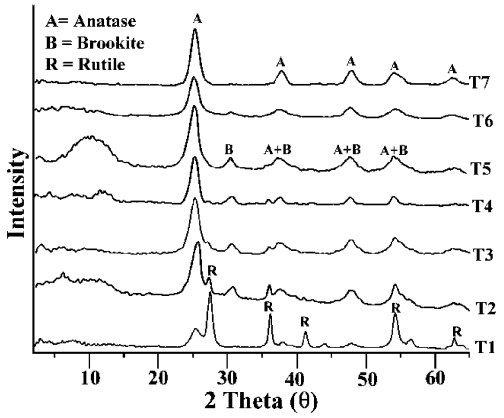

Figure 1. XRD pattern of TiO_2 nanocrystals prepared by thermal hydrolysis of $TiCl_4$ in mixed water ethanol solvent with varying water to ethanol volume ratio.

volume ratios. It is observed that a mixture of nanocrystalline titania consisting of rutile/brookite, anatase/brookite and phase-pure anatase were obtained in the mixed solvent system with controlled variation in water to ethanol volume ratio. In the absence of ethanol as in the case of sample T1, the addition of $TiCl_4$ directly to pure water results in a white precipitate formed almost instantaneously, which was a mixture of both rutile and anatase. The characterized sample was ~75:25 mix of rutile (JCPDS file no. 21−1276) and anatase phase (JCPDS file no. 21−1272). The intermediate systems, such as, T2, T3, T4, and T5 yielded predominantly brookite (JCPDS file no. 2−514) in considerable amount with mixed presence of either rutile or anatase. The fraction of rutile is found to decrease with increasing ethanol content. On the contrary, presence of brookite initially increases and then decreases steadily while

Table 1. Quantitative Phase Composition and Crystallite Diameters of Nanocrystalline TiO_2 Prepared by Thermolysis of the $TiCl_4$ Precursor at 100 °C for 16 h in Mixed Water Ethanol Solvent Media with Different Volume Ratios

sample ID	water to ethanol ratio (v/v)	rutile (wt %)	anatase (wt %)	brookite (wt %)	d_{rutile} (nm)	$d_{anatase}$ (nm)	$d_{brookite}$ (nm)	ref
T1	70:0	75.7	24.3		9.1	4.61		31
T2	60:10	32.3		67.7	7.2		5.2	15
T3	50:20	16.3		83.7	5.72		5.2	15
T4	40:30		24.3	75.7			5.23	19, 24
T5	30:40		36.7	63.3		5.38	6.14	14, 24
T6	20:50		71	29		5.63	7.3	14, 24
T7	10:60		100			5.89		24, 28

anatase starts to reappear with decreasing water content in the mixed solvent system. The intensity of the anatase peak significantly increases with volume fraction of ethanol concentration, finally leading to phase pure anatase in water: ethanol ratio of 1:6. The results show that increasing concentration of ethanol leads to phase pure anatase suggesting that higher ethanol content preferentially leads to form anatase phase.[18] Because of the peak overlap in XRD at $2\theta = 25.7°$ for both anatase (101) and two brookite planes, (111), (120), the existence of brookite phase was ascertained by the presence of its (121) plane indexed at 30.9° in the XRD profiles obtained. In contrast, a mixture of anatase and brookite (JCPDS file no. 76−1935) TiO_2 phases is observed in sample T5.

The average crystallite sizes of anatase, rutile, and brookite were estimated by applying the Scherrer's equation to the major peaks of the diffraction data and taking an average.

$$D = \frac{K\lambda}{\beta\cos\theta} \quad (1)$$

Where D is the average crystallite size obtained in angstroms (Å) and K is the shape factor taken as 0.9, λ is the wavelength of X-ray radiation (Cu Kα = 1.5406 Å), β is the full width at half-maximum after making appropriate baseline correction and θ is the diffraction angle. The phase composition of TiO_2 can be estimated from the integral intensities of anatase (101) peak, rutile (110) peak and brookite (121) peak using the equation reported by Zhang et al. with optimized coefficients k_A and k_B as 0.886 and 2.217, respectively.[19] The phase compositions and crystallite sizes of the samples are summarized in Table 1. All synthesized samples were nanocrystalline and the dimensions range from ∼4−10 nm. In each mixture, the crystallite size of anatase and brookite was always found to be lower than that of rutile. With the increase in ethanol concentration, however, the estimated crystallite size is observed to decrease for rutile whereas for anatase and brookite, it increases steadily.

Raman spectroscopy is a very sensitive tool to assess the phase purity and crystallinity of TiO_2. The phase transition and existence of large amount of brookite and phase pure anatase was further confirmed by Raman analysis. Anatase exhibits characteristic scatterings at 146 cm^{-1} (E_g), 396 cm^{-1} (B_{1g}), 516 cm^{-1} (A_{1g}) and 641 cm^{-1} (E_g),[20] and brookite shows sharp peaks at 128 cm^{-1} (A_{1g}), 153 cm^{-1} (A_{1g}), 247 cm^{-1} (A_{1g}), 322 cm^{-1} (B_{1g}), 366 (B_{2g}), and 636 cm^{-1} (A_{1g}),[21] while rutile gives typical scatterings at 143 cm^{-1} (B_{1g}), 235 cm^{-1}, 447 cm^{-1} (E_g), and 612 cm^{-1} (A_{1g}).[22] Figure 2 shows Raman spectra of the three representative samples T3, T5, and T7. The observed peak position of the Raman bands are in good accordance with the documented literature data.[23,24] Slight shift of peak position observed for the samples T3 and T5 in the region 100−200 cm^{-1} as depicted in the inset, is believed to be due to the close proximity to the predominantly brookite phase.[25] For the

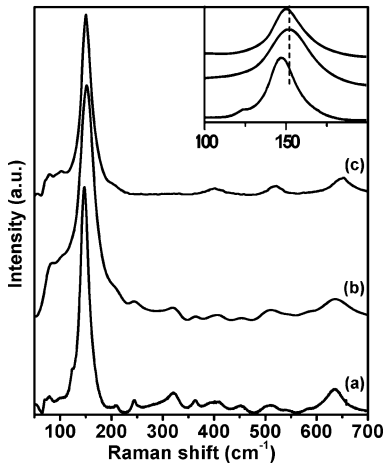

Figure 2. Raman spectra of the mixed phase nanocrystalline TiO_2 with different phase composition: (a) T3, (b) T5, and (c) T7. Corresponding inset show the peak shift due to the mixed composition.

sample, T3, which consists of 17% of rutile and 83% brookite, the presence of the rutile phase is confirmed from the peak appearing at 449 cm^{-1}. In the case of sample, T5, which is a mixture of brookite and anatase phases, a shift in the peak positions is observed for the peaks corresponding to the anatase, whereas the peaks pertaining to brookite appear at their designated position.

Morphology and average particle size of the synthesized nanocrystalline TiO_2 are investigated by transmission electron microscopy. Figure 3 shows the TEM images of mixed phase TiO_2 synthesized at constant temperature and $TiCl_4$ concentration. As shown in Figure 3, T1 and T2 are composed of nanorods with some nanoparticles observed on the surface of these nanorods. This observation strongly indicates the presence of different crystalline polymorphs in the images of T1 and T2, and conforms to the XRD analysis. Although the presence of nanorods is noticeably less visible in T2, it is clear that the small spheroidal aggregates that appear are of predominately one polymorph. This evidence and comparative evaluation on the basis of the XRD along with the TEM results, leads us to deduce that the nanorods and nanoparticles can be ascribed to the rutile and brookite phases, respectively. However, it is increasingly difficult to detect the presence of nanorods in the case of samples T3, where the percentage of rutile contribution falls down significantly. The high resolution TEM and SAED images of sample T3 (Figure 3h) reveals that nanoparticles are well crystalline and indicates the presence of large amount of brookite phase. The lattice spacing (depicted in Figure 3h) of nanoparticles is 0.349 and 0.291 nm, corresponding to the crystal planes of brookite, (111) and

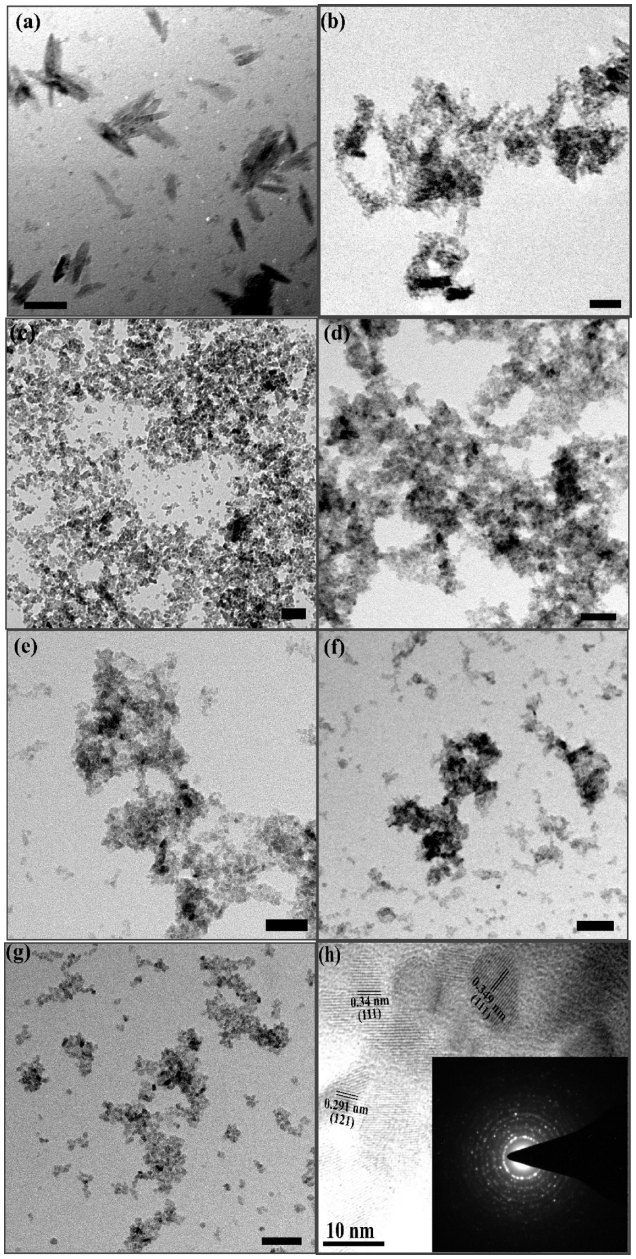

Figure 3. TEM images of as prepared TiO_2 nanocrystals: (a) T1, (b) T2, (c) T3, (d) T4, (e) T5, (f) T6, and (g) T7. Scale bar is 50 nm in a–g. (h) HRTEM image and SAED (inset) pattern of sample T3.

(121), respectively. When ethanol concentration is increased (T6, T7) in the reaction medium the particles remain spherical in nature, with a slight increase in the particles size, but unlike rutile (spindle/nanorod-like structure), the presence of increasing amounts of anatase in the system could not be ascertained on the basis of the morphology. The samples are characterized further for estimation of their specific surface area by BET method and these results are tabulated in Table 2. High surface area of mixed phase TiO_2 was attributed to low temperature hydrolysis method resulting in smaller size of the nanoparticles synthesized. It can be inferred that the surface area down the synthesized series (T1 → T7) for mixed-phase nanocrystalline TiO_2 can be attributed to decrease in the agglomeration of TiO_2 nanoparticles. This possibly suggests that increasing the concentration of ethanol in reaction medium

Table 2. Physicochemical Parameters of As Synthesized Samples and Photocatalytic Degradation Rate Constant Values

sample ID	band gap[a] (eV)	BET $m^2\ g^{-1}$	rate constant[b] k (min^{-1})
T1	3.02	135.64	0.018
T2	3.17	140.88	0.025
T3	3.17	163.9	0.041
T4	3.24	164.3	0.031
T5	3.24	205.82	0.038
T6	3.25	222.2	0.033
T7	3.31	245.1	0.032
P25			0.028

[a]Calculated from eq 2. [b]Calculated from eq 3.

may lead to partial stabilization of surface energy and hence lower agglomeration and an increase in the surface area.

3.1. Photo-Absorption Measurement. Figure 4 depicts typical UV–vis absorption spectra of mixed phase nanocrystal-

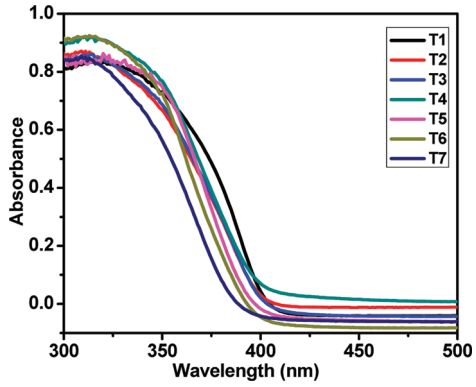

Figure 4. Diffuse reflectance absorption spectra of as synthesized samples.

line TiO_2 with varying phase content. The optical absorption edges were found to be in the range of 378–411 nm and the optical band gap was estimated using the equation.

$$E = hc/\lambda \quad (2)$$

where h is Plank's constant (6.625×10^{-34} J s), c is the velocity of light in vacuum (3×10^8 m s^{-1}), and λ is wavelength corresponding to the intersection of the band edge (linear portion of the absorption slope) on the x-axis.[6] For the phase pure anatase, the absorption wavelength at 378 nm, a band gap value at 3.31 eV is exhibited, which is in good accordance with reported literature data.[26] The mixed phase TiO_2 sample, T1 containing 76% of rutile shows significant absorption at 411 nm, gives a corresponding value of 3.02 eV, which is also close to that obtained for phase-pure rutile TiO_2.[27] Interestingly, in the the absorption spectra (Figure 4), a steady blue shift is also observed clearly for the intermediate samples in the series. This shift in absorption edge toward lower wavelength is implicit of the decreasing rutile content. In absence of any documented experimental data available for the optical band gap of phase pure brookite, different opinions are reported in literature. Although it is estimated that the optical band gap of brookite is ~0.46 and ~0.16 eV higher than that of rutile and anatase phase, respectively;[28] some reports indicate that it lies in-between those of anatase and rutile.[24] Our present studies on biphasic samples indicate that it may indeed be positioned in

dx.doi.org/10.1021/am201354r | ACS Appl. Mater. Interfaces 2012, 4, 1239–1246

between that of rutile and anatase. The relatively larger band gap values observed in our samples when compared to that of phase-pure rutile could probably be attributed to the initial contribution of brookite and thereafter steadily increasing surface area and anatase content. Additionally, the quantum size effect is also presumed to contribute significantly in the observed large band gap for the synthesized samples. To sum up, it is clear that the optical band gap results are consistent with varying phase content and the percent dominant phase has major influence on the estimated values.

3.2. Photoactivity. The photoactivity of all the synthesized samples and Degussa P-25 used as reference were investigated by studying the degradation kinetics of RhB under visible light is represented in Figure 5. The photocatalytic efficiency of the

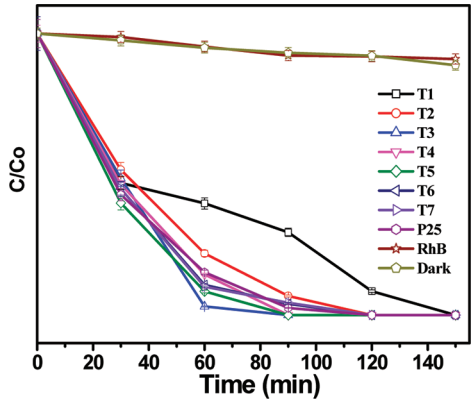

Figure 5. C/C_O verses Time for the degradation of RhB under visible light. C_O and C are the initial concentration after the adsorption equilibrium and the concentration of RhB at different photo-degradation times, respectively.

studied samples as listed in Table 2, can be classified under pseudofirst-order, where the rate and the kinetic equation can be expressed as

$$Kt = \ln \frac{C_o}{C_t} \qquad (3)$$

The synthesized samples exhibit different photoactivities depending on their phase composition and surface area. It is found among all the TiO_2 samples tested, T3, consisting of 83% of brookite and 17% of rutile shows the best performance in terms of photoactivity toward the degradation of RhB. Except for samples T1and T2, the mixed-phase catalyst performance was superior and they were comparable to or even better than P25. The order of photocatalytic activities in the samples studied can be represented as T3 > T5 > T7 = T6 > T4 > P25 > T2 > T1, and the corresponding degradation rate constants calculated are listed in Table 2. Although T7, which is phase pure anatase, possesses higher surface area (245.1 $m^2\ g^{-1}$) among all the synthesized samples, the activity of T3 was found to be superior compared to P25 and definitely better than phase-pure anatase. This particular observation supported with previous reports on mixed phase activity[15] leads us to conclusively believe that surface area is not the only factor that determines the photoactivity. In the case of mixed-phase TiO_2, the brookite to rutile ratio might be a more determining factor for the high photoactivity observed. This argument is strengthened by the fact that samples T2 and T3 both consist of brookite and rutile phase, however, the significant difference in photoactivities clearly suggests that tuning the brookite to rutile ratio, the photocatalytic efficiency of mixed phase TiO_2 can be appropriately controlled. In case, there is no interactions/junctions formed between brookite and rutile nanoparticles, then the photoactivity depends on the individual crystal phase.[11,15] However, because in the present synthetic procedure both the phases are formed in situ, and not a mere physical blend of two different phases, this interaction between the brookite and rutile nanoparticles is plausible and a facile irreversible charge transfer from one phase to another promotes the photocatalytic efficiency.

Under visible light irradiation, RhB dye generates excited singlet states and sensitizes the mixed titania phases (Figure 7).

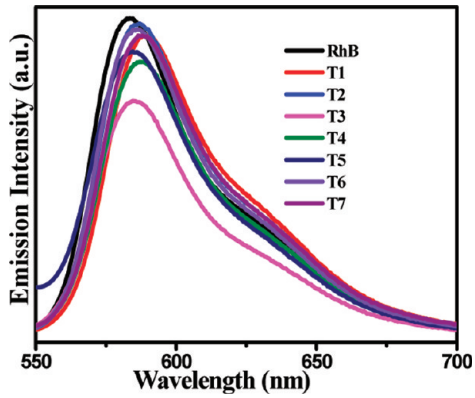

Figure 6. Photoluminescence spectra of Rhodamine B in presence of the as-synthesized samples.

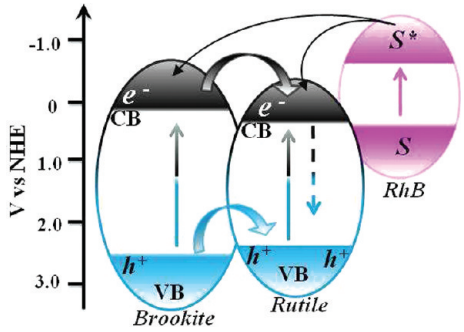

Figure 7. Schematic representation of possible electron–hole separation mechanism proposed for mixed phase nanocrystals during photocatalysis. The difference between band edges of two phases allows migrating photogenerated holes and electrons across the interface.

The photoexcited electron facilitated by interfacial electron transfer, migrates from higher conduction band of brookite to slightly lower conduction band of rutile, whereas the excited electrons in the rutile cannot migrate to the brookite phase.[28,29] Correspondingly, the valence band edge of rutile is found to be slightly higher in energy than the brookite. It has been proposed that the holes migrate much faster than electrons,[30] and therefore the holes can migrate toward the rutile phase resulting in longer lifetimes of the conduction band electrons residing in the brookite phase.[31] Hence, an increase in the holes in rutile and a concurrent decrease in holes in brookite under light irradiation can create a effective charge separation . This will in effect reduce recombination of photogenerated electrons

dx.doi.org/10.1021/am201354r | ACS Appl. Mater. Interfaces 2012, 4, 1239–1246

and holes in the brookite phase and consequently improve the photocatalytic efficiency of this phase.[14,28]

A similar argument can well be extended to the other mixed anatase-brookite phase samples, however, with reduced efficiency primarily due to the similarity in crystal structure. For example, sample T5 on the one hand also shows higher photoactivity than phase-pure anatase (T7) and P25, but slightly less than T3. This lower photoactivity in comparison with rutile/brookite mixture can be rationalized on the following lines. The electronic structure of brookite is analogous to that of anatase with only minor differences in the local crystal environment between the two phases.[28] The similarity between the two phases and band gap leads to a comparable decrease in the efficiency of electron−hole pair separation process at the junction. Nonetheless, it has been demonstrated earlier that a high percentage composition of brookite in anatase mixture can attribute to fairly high photoactivity.[14] Our results also confirm this fact, that the sample (T5) containing 63% of brookite exhibits a better photoactivity than sample (T6) containing 28% of brookite. It can therefore be said that brookite ratio is the most important factor for the high photoactivity among the synthesized samples.

The aim of developing mixed phase TiO_2 is to modify the kinetics of recombination for the photoexcited electrons and holes, in such a way so as to improve the catalytic performance. These electrons and holes are primarily responsible for the generation of hydroxide radical and O_2^- reactive species.[31] In this process, rate of separation and recombination of light induced charge carriers can be gauged by the luminescence intensity. According to literature reports, the photoluminescence of TiO_2 is weak and sensitive at room temperature.[32] Hence, to assess the nature of the degradation of RhB under visible light, we have analyzed the luminescence spectra of RhB in presence of TiO_2, depicted in Figure 6. The results indicate that, the emission of RhB varies as a function of the phase composition of TiO_2. Noticeably, with an increase in brookite content of the system, the luminescence of RhB decreases, which strongly supports the proposed argument of the correlated interfacial charge transfer events and effective charge separation in biphasic samples. As observed, the photoluminescence spectra for phase composition, T3, is found to be significantly suppressed, indicating enhanced interactions between the RhB and biphasic titania.

It must be mentioned that the synthesis of phase pure anatase, rutile and brookite by thermal hydrolysis of $TiCl_4$ was strongly affected by the acid medium and nature of anions upon the thermolysis.[33,34] Agatino Di Paola et al. reported binary or ternary mixture of the three polymorphs of TiO_2 predominately obtained by thermal hydrolysis of $TiCl_4$ in water at 100 °C by tuning the $TiCl_4$ to H_2O ratio.[35] They suggested that water and $TiCl_4$, concentrations of both are important parameters to determine the crystal phases of TiO_2 formed. Yawen et al. examined the effect of $C_2H_5O^-$ ion on hydrolysis of $TiCl_4$ in aqueous ethanol at 50 °C under hydrothermal condition.[36] In the present investigation, we examine the effect of mixed solvent compositions for thermal hydrolysis and found that ethanol plays an important factor in determining the crystalline structure of TiO_2 at 100 °C.

All the three polymorphs of TiO_2 are grown from TiO_6 octahedra and phase formation differs only due to the nature of sharing corners or edges. There are four shared edges for octahedron in anatase, three in brookite, and two in rutile. The structure of brookite has both shared edges and corners, a compromise between anatase and rutile in terms of shared faces.[24] Aruna et al. ruled out that structure of the precursor cation is affected by pH of solution.[37] The effect of variable pH for the study can be safely taken out of consideration as the pH of the milli-Q water and absolute ethanol used is approximately equal.

Under the hydrolytic reaction conditions, $TiCl_4$ exhibits strong tendency to form $[Ti(OH)_nCl_m(OH_2)_{6-n-m}]^{(n+m-4)-}$ complex and generates hydrochloric acid. Rutile can be developed through the corner shared bonding along the [001] direction by the dehydration of OH ligand in $[Ti(OH)_nCl_m(OC_2H_5)_{6-n-m}]^{(n+m-4)-}$ complex in highly acidic medium. The effect of hydrochloric acid has been investigated extensively, and it is well-established that rutile formation is more thermodynamically favorable under acidic condition.[38] Brookite, a metastable phase, is normally obtained under thermal treatment at considerably lower temperatures. Thus, acidic conditions also favors the formation of brookite phase mediated by a non-electrically charged $[Ti(OH)_2Cl_2(OH_2)_2]^O$ transition complex.[38] This argument holds good to explain the formation of predominantly brookite phase in the present study. In water−ethanol mixture, metal precursor $TiCl_4$ hydrolyzes to form a 6-fold coordinated $[Ti(OH)_nCl_m(OC_2H_5)_{6-n-m}]^{(n+m-4)-}$ complex species and HCl, where n and m are associated with the acidity and $[Cl^-]$ in the reaction system, respectively.[36] With addition of ethanol, the chloride ligands from the $[Ti(OH)_nCl_m(OC_2H_5)_{6-n-m}]^{(n+m-4)-}$ complex are progressively eliminated. The excess Cl^- ions in the reaction system can act as structure directing agent for the growth of brookite phase under these conditions. The presence of $C_2H_5O^-$ in the medium serves as a barrier against the instantaneous hydrolysis of $TiCl_4$ and effectively helps to control the rate of hydrolysis thus favoring the formation of large quantities of brookite.[35] The rational may well be one of the reason for no product formation when absolute ethanol media was used. Furthermore, ethanol facilitates the formation of spherical nanoparticles and lowers agglomeration by effectively acting as a surface stabilizing agent. As the ethanol composition for the mixed solvent system increases, more $C_2H_5O^-$ anions are available compared to the Cl^- ions in the reaction system. Thus, the structure directing role of Cl^- ion is minimized to a large extent. The crystallites of TiO_2 formed naturally carry surface positive charge under acidic conditions.[39,40] Unlike Cl^- as structure directing agent, the bulkier $C_2H_5O^-$ anions adsorbed on Ti^{4+} cations precludes the corner sharing and facilitate the edge sharing, yielding finer anatase crystallites. It is also accepted that the relative stability of TiO_2 polymorph is size dependent, anatase is the most stable at sizes below 11 nm, whereas brookite is ∼11−35 nm. Reduction in size for brookite leads to destabilization and recrystallization into anatase phase.[19]In this work, the brookite crystallite size in the mixture of TiO_2 is less than ∼8 nm.

To substantiate the proposed mechanism of formation and rationalize the effect of the solvent on the reaction system studied, we carried out pH measurements pre- and post-synthesis (see the Supporting Information, Table 1). As compared in the table, concentration of H^+ ions slightly increased as hydrolysis proceeds in water.[41] In mixed solvent media, the amount of solvated HCl could decrease because of poor solubility in ethanol when compared to water and the undissolved HCl is released out.[42] As observed postsynthesis for the system T1, HCl gas released in situ is soluble in water,

so the pH of the reaction system decreases, and the change is quite significant. These highly acidic conditions as well as large concentration of Cl^- ions are favored for preferential formation of rutile phase with small amount of anatase or brookite. On increasing ethanol content, the partial decrease of HCl solubility in the medium affects the availability of Cl^- ions, which plays an important structure directing role for the formation of rutile. Consequently, the fraction of rutile phase decreases as observed from XRD and Raman studies. When substantial quantity of ethanol is used, pH change observed is not so considerable. The low availability of Cl^- ions in the system manifests itself in the form of preferential formation of anatase, as in the case of the system T7.

CONCLUSION

In summary, we have developed a simple method to synthesize enhanced photoactivity in mixed-phase nanocrystalline titanium dioxide photo catalyst with tunable phase composition by thermal hydrolysis of titanium tetrachloride in the presence of aqueous ethanol. By changing the water to ethanol ratio, we easily tune the ratio of rutile to brookite and brookite to anatase. The samples were nanocrystalline and possess large surface area. The photcatalytic measurement results show that the synthesized samples exhibit high photoactivity. Among all samples, the sample containing 17% rutile and 83% brookite exhibits the highest photoactivity, higher than P25 and better than phase-pure anatase. The improved performance could be explained by synergetic effect, which is caused by the increasing charge separation efficiency resulting from interfacial electron transfer from one phase to another.

ASSOCIATED CONTENT

Supporting Information

Additional figures (PDF). This material is available free of charge via the Internet at http://pubs.acs.org.

AUTHOR INFORMATION

Corresponding Author

*E-mail: manorama@iict.res.in. Tel: +91-40-27193225. Fax: +91-40-27160921.

Notes

The authors declare no competing financial interest.

ACKNOWLEDGMENTS

B.R.R. acknowledges UGC for the grant of fellowship, P.B. acknowledges DST for the Ramanujan Fellowship, and all the authors acknowledge the financial support from the Indo-NIMS project under which this work was carried out. We appreciate the help from University Of Hyderabad TEM facility for providing HRTEM images. The help extended by Dr. L. Giribabu and Mr. U. V. R. Sharma for the PL and LC measurements is duly acknowledged.

REFERENCES

(1) O'Regan, B.; Graetzel, M. *Nature* **1991**, *353*, 737−740.
(2) Tryk, D. A.; Fujishima, A.; Honda, K. *Electrochim. Acta* **2000**, *45*, 2363−2376.
(3) Linsebigler, A. L.; Guangqan, L.; Yates, J. T. *Chem. Rev.* **1995**, *95*, 735−758.
(4) Kato, K.; Tsuzuki, A.; Taoda, H.; Torii, Y.; Kato, T.; Butsugan, Y. *J. Mater. Sci.* **1994**, *29*, 5911−5915.
(5) Bakardjieva, S.; Subrt, J.; Stengl, V.; Vecernikova, E.; Bezdicka, P. *Solid State Phenom.* **2003**, *7*, 90−91.
(6) Zachariah, A.; Baiju, K. V.; Shukla, S.; Deepa, K. S.; James, J.; Warrier, K. G. K. *J. Phys. Chem. C* **2008**, *112*, 11345−11356.
(7) Ding, Z.; Lu, G. Q.; Greenfield, P. F. *J. Phys. Chem. B* **2000**, *104*, 4815−4820.
(8) Nagaveni, K.; Sivalingam, G.; Hedge, M. S.; Madras, G. *Appl. Catal. B Environ.* **2004**, *48*, 83−93.
(9) Kolar, M.; Mest Ankova, H.; Jirkovsky, J.; Heyrovsky, M.; Subrt, J. *Langmuir* **2006**, *22*, 598−604.
(10) Ohno, T.; Tokieda, K.; Higashida, S.; Matsumura, M. *Appl. Catal., A* **2003**, *244*, 383−391.
(11) Kawahara, T.; Konishi, Y.; Tada, H.; Tohge, N.; Nishii, J.; Ito, S. *Angew. Chem., Int. Ed.* **2002**, *41*, 2811−2813.
(12) Bickley, R. J. *J. Solid State Chem.* **1991**, *92*, 178−190.
(13) Wenjun, Z.; Xiaodi, L.; Zhiying, Y.; Lianjie, Z. *AcsNano* **2009**, *3*, 155−122.
(14) Yu, J. C.; Lizhi, Z.; Jiaguo, Y. *Chem. Mater.* **2002**, *14*, 4647−4653.
(15) Hua, X.; Lizhi, Z. *J. Phys. Chem. C* **2009**, *113*, 1785−1790.
(16) Jinghuan, Z.; Xin, X.; Junmin, N. *J. Hazard. Mater.* **2010**, *176*, 617−622.
(17) Ohtani, B.; Handa, J. I.; Nishimoto, S. I.; Kagiya, T. *Chem. Phys.Lett.* **1985**, *120*, 292−294.
(18) She, L.; Weng, D. *J. Environ. Sci.* **2008**, *20*, 1263−1267.
(19) Zhang, H.; Banfield, J. F. *J. Phys. Chem. B* **2000**, *104*, 3481−3487.
(20) Ohsaka, T.; Izumi, F.; Fujiki, Y. *J. Raman Spectrosc.* **1978**, *7*, 321−324.
(21) Tompsett, G. A.; Bowmaker, G. A.; Cooney, R. P.; Metson, J. B.; Rogers, K. A.; Seakins, J. M. *J. Raman Spectrosc.* **1995**, *26*, 57−62.
(22) Chaves, A.; Katiyan, K. S.; Porto, S. P. S *Phys. Rev.* **1974**, *10*, 3522−3533.
(23) Raffaella, B.; Vincenzo, G.; Elvio, C.; Cinzia, G.; Tobias, K.; Roberto, C.; Pantaleo, D. C. *J. Am. Chem. Soc.* **2008**, *130*, 11223−11233.
(24) Ji-Guang, Li.; Takamasa, I.; Xudong, S. *J. Phys. Chem. C* **2007**, *111*, 4969−4976.
(25) Kandiel, T. A.; Armin, F.; Lars, R.; Ralf, D.; Bahnemann, D. W. *Chem. Mater.* **2010**, *22*, 2050−2060.
(26) Maocheng, Y.; Feng, C.; Jinlong, Z.; Masakazu, A. *J. Phys. Chem. B* **2005**, *109*, 8673−8678.
(27) Hoffmann, M. R.; Martin, S. T.; Choi, W.; Bahnemann, D. W. *Chem. Rev.* **1995**, *95*, 69−96.
(28) Dongjiang, Y.; Hongwei, L.; Zhanfeng, Z.; Yong, Y.; Jin-cai, Z.; Waclawik, E. R.; Xuebin, K.; Huaiyong, Z. *J. Am. Chem. Soc.* **2009**, *131*, 17885−17893.
(29) Zachariah, A.; Baiju, K. V.; Shukla, S.; Deepa, K. S.; James, J.; Warrier, K. G. K. *J. Phys. Chem. C* **2008**, *112*, 11345−11356.
(30) Enright, B.; Fitzmaurice, D. *J. Phys. Chem.* **1996**, *100*, 1027−1035.
(31) Joana, T. C.; Savenije, T. J.; Moulijn, J. A.; Guido, M. *J. Phys. Chem. C* **2011**, *115*, 2211−2217.
(32) Sreejith, K.; Ghosh, H. N. *J. Mater. Chem.* **2009**, *19*, 3523−3528.
(33) Yin, H. B.; Wada, Y.; Kitamura, T.; Sumida, T.; Hasegawa, Y.; Yanagida, S. *J. Mater. Chem.* **2002**, *12*, 378−383.
(34) Cassaignon, S.; Koelsch, M.; Jolivet, J. P. *J. Mater. Sci.* **2007**, *42*, 6689−6695.
(35) Agatino, D. P.; Marianna, B.; Riccardo, C.; Leonardo, P.; Francesco, P. *J. Phys. Chem. C* **2009**, *113*, 15166−15174.
(36) Yawen, W.; Lizhi, Z.; Kejian, D.; Xinyi, C.; Zhigang, Z. *J. Phys. Chem. C* **2007**, *111*, 2709−2714.
(37) Aruna, S. T.; Tirosh, S.; Zaban, A. *J. Mater. Chem.* **2000**, *10*, 2388−2391.
(38) Pottier, A.; Chanéac, C.; Tronc, E.; Mazerolles, L.; Jolivet, J.-P. *J. Mater. Chem.* **2001**, *11*, 1116−1121.
(39) Matijevic, E. *J. Colloid Interface Sci.* **1977**, *58*, 374−389.
(40) Sugimoto, T. *Adv. Colloid Interface Sci.* **1987**, *28*, 65−108.
(41) Yuanzhi, L.; Yining, F.; Chen, Y. *J. Mater. Chem.* **2002**, *12*, 1387−1390.

(42) Hongmei, L.; Cheng, W.; Yushan, Y. *Chem. Mater.* **2003**, *15*, 3841−3846.